Anchoring of Vanadyl Acetylacetonate onto Amine-Functionalised Activated Carbons: Catalytic Activity in the Epoxidation of an Allylic Alcohol

Bruno Jarrais,[a] Ana Rosa Silva,[a] and Cristina Freire*[a]

Keywords: Activated carbon / Anchoring / Epoxidation / EPR spectroscopy / Vanadium

Vanadyl(IV) acetylacetonate was anchored onto two different amine-functionalised activated carbons. The starting activated carbon supports were air (A2) and nitric acid oxidised (B1) carbons; the phenol surface groups of carbon A2 were subsequently treated with (3-aminopropyl)triethoxysilane (A3) and afterwards the free amine groups were used for Schiff condensation with $[VO(acac)_2]$ (A4). Carbon B1, which possesses carboxylic surface groups, was treated with thionyl chloride to give surface acyl chloride groups (B2), which were then reacted with the amine groups of bis(3-aminopropyl)amine (B3); subsequent attachment of $[VO(acac)_2]$ was also achieved by Schiff condensation between the free amine groups of the functionalised carbon and the ligand oxygen atoms (B4). All the materials were characterised by XPS, and the $[VO(acac)_2]$-based materials were also characterised by vanadium elemental analysis and EPR spectroscopy. A combination of all the data provides evidence for the covalent attachment of the vanadium complex onto the modified activated carbons. The catalytic activity of the $[VO(acac)_2]$-based materials in the epoxidation of 3-buten-2-ol using *tert*-butyl hydroperoxide as oxygen source was assessed and compared to that of the homogeneous phase reaction. The alkene conversion in the heterogeneous phase is similar to that observed in the homogeneous phase, although the rate of oxidation is less than half that of the homogeneous system. Material A4 exhibits higher catalytic efficiency than B4; upon reuse, both materials show no significant decrease in their catalytic properties.

Introduction

Vanadyl(IV) acetylacetonate has been found to be a useful homogeneous catalyst in several oxidation reactions, such as the oxidation of alcohols,[1] oxidation of sulfides to sufoxides,[1,2] oxidation of thiols to disulfides[3] and in the epoxidation of allylic alcohols.[1,2] Moreover, the catalytic activity of vanadyl(IV) acetylacetonate is not only restricted to oxidation reactions; it has also been employed in ring-cleavage reactions[4] and in oxidative polymerisation reactions[5] and polymerisation of diphenyl disulfides,[6] thus making it a versatile and readily available catalyst.

Epoxides are extremely useful building blocks in the synthesis of organic compounds as they act as excellent intermediates that can yield a great variety of products.[7] The homogeneous epoxidation of allylic alcohols by vanadyl(IV) acetylacetonate under mild conditions and using *tert*-butyl hydroperoxide as the oxygen source has been widely studied and exhibits high activity, selectivity and regioselectivity.[1,2,8,9] The catalytically active oxo-peroxo intermediate is formed in situ by oxidation of V^{IV} to V^{V} with an excess of *tert*-butyl hydroperoxide, yielding a *tert*-butyl hydroperoxovanadium(V) complex. A good example of the high regioselectivity of this complex is the epoxidation of geraniol, an allylic alcohol containing an isolated double bond, which is catalysed by a $[VO(acac)_2]$–*tert*-butyl hydroperoxide system, where the allylic double bond is selectively oxidised, whereas peracids preferentially epoxidise the isolated double bond.[1]

The heterogenisation of these transition metal complexes on solid supports allows the combination of their homogeneous catalytic properties with those of heterogeneous catalysts, such as the ease of separation from reaction media, shape selectivity and reuseability.[10–13] Early approaches to heterogenisation consisted of ion exchanging or simple adsorption of the metal complexes onto the supports, but these procedures did not prevent active-phase leaching.[12,13] This problem was recently overcome by the development of several grafting and tethering methodologies, which allow the covalent attachment of transition metal complexes to organic polymers, silica, zeolites and other micro- and mesoporous inorganic materials.[10–13]

Activated carbons and other carbon-based materials are widely used as catalysts and as supports for metals in their reduced state,[14,15] and a few reports have appeared on the heterogenisation of metal complexes, mainly of noble metals with simple ligands, to be used in hydrogenation and hydroformylation reactions.[16–18] We have been developing several anchoring procedures to immobilise Schiff-base transition metal complexes onto activated carbons and

[a] REQUIMTE, Departamento de Química, Faculdade de Ciências, Universidade do Porto,
4169-007 Porto, Portugal
Fax: +351-22-608-2959
E-mail: acfreire@fc.up.pt

  DOI: 10.1002/ejic.200500435

other supports.[19–23] In one of these works, copper(II) acetylacetonate was irreversibly anchored onto a chemically oxidised activated carbon functionalised with bis(3-aminopropyl)amine (trien) by Schiff-base condensation between the free amine groups of trien covalently attached to the activated carbon surface and the oxygen atoms of acetylacetonate coordinated to copper(II).[23] In the present work, we report an extension of this latter procedure to vanadyl(IV) acetylacetonate and a new route for complex immobilisation, in which an oxygen-oxidised activated carbon, previously functionalised with (3-aminopropyl)triethoxysilane (APTES), is used to anchor vanadyl(IV) acetylacetonate by Schiff-base condensation between the free amine groups of APTES and the ligand oxygen atoms. The functionalisation steps were followed by X-ray photoelectron spectroscopy (XPS), and the $[VO(acac)_2]$-based materials were characterised by vanadium ICP-AES analysis and by EPR spectroscopy. The catalytic activity of these two novel carbon-based vanadyl(IV) acetylacetonate heterogeneous catalysts was tested at 0 °C in the epoxidation of an allylic alcohol (3-buten-2-ol) in dichloromethane using *tert*-butyl hydroperoxide (*t*BuOOH) as the oxygen source. Their reusability was also tested.

Results and Discussion

Vanadyl(IV) acetylacetonate was anchored onto two different amine-functionalised activated carbons using the methods summarised in Scheme 1. In method A, an air-oxidised activated carbon (A2) with a high amount of surface phenol groups was treated with (3-aminopropyl)triethoxysilane (APTES), resulting in a surface with free amine groups (A3). In method B, the starting material was a nitric acid oxidised activated carbon (B1), which possesses a high concentration of carboxylic acid groups. These were converted into more reactive acyl chloride functionalities by treatment with thionyl chloride (B2), and then reacted with the amine groups of bis(3-aminopropyl)amine (trien, B3). The free amine groups in both carbons A3 and B3 were used for Schiff-base condensation with $[VO(acac)_2]$ to give A4 and B4, respectively. All the materials were characterised by XPS, and the $[VO(acac)_2]$-based materials were also characterised by vanadium ICP-AES analysis and EPR spectroscopy. The XPS data of materials A1, A2, B1, B2 and B3 have already been described in previous papers[22,23] and thus here we will focus on the characterisation of the new materials, only recalling relevant aspects of the previous ones.

Characterisation of the Heterogeneous Catalysts

X-ray Photoelectron Spectroscopy and Elemental Analysis

Table 1 contains the XPS atomic percentages of all the carbon-based materials and Figure 1 shows the XPS high-resolution spectra in the O 1s region (for the series of carbons A) and in the V 2p region (for carbons with anchored vanadyl complexes, A4 and B4).

Table 1. XPS atomic percentages for carbon-based materials.

Sample	Atom %						Ref.
	O	N	Cl	C	Si	V	
A1	7.66	0.58	0.86	90.41	–	–	this work
A2	12.58	0.70	0.30	86.15	–	–	this work
A3	17.08	2.83	–	73.44	6.66	–	this work
A4	17.71	2.55	0.23	73.24	5.28	0.98	this work
B1	20.27	0.58	0.13	78.61	[a]	–	[23]
B2	10.98	0.60	3.03	84.84	[a]	–	[23]
B3	9.01	3.64	1.81	85.06	[a]	–	[23]
B4	8.56	2.07	1.05	87.10	0.49[b]	0.72	this work

[a] Not analysed. [b] Silica impurity on carbon matrix.

There is a significant increase in the oxygen content when the parent carbon A1 is submitted to the two different oxidation procedures (Table 1), thus indicating the formation of new oxygen functionalities at the surface of the activated carbon.[19–24]

In the O 1s region (Figure 1, a), sample A1 exhibits a symmetrical broad peak centred at 532.3 eV, whereas sample A2 shows a more-intense and asymmetric peak centred at 533.6 eV with a shoulder at 532.0 eV. The air oxidation of A1 increases the number of phenol and carbonyl groups,[24] which exhibit O 1s peaks in the region 532–533 eV,[25–27] therefore the shoulder in A2 is assigned to these basic groups. After reaction with APTES (A3), there is an increase in the area under the bands in the N 1s, O 1s and Si 2p regions, as can be seen in Table 1, thus confirming

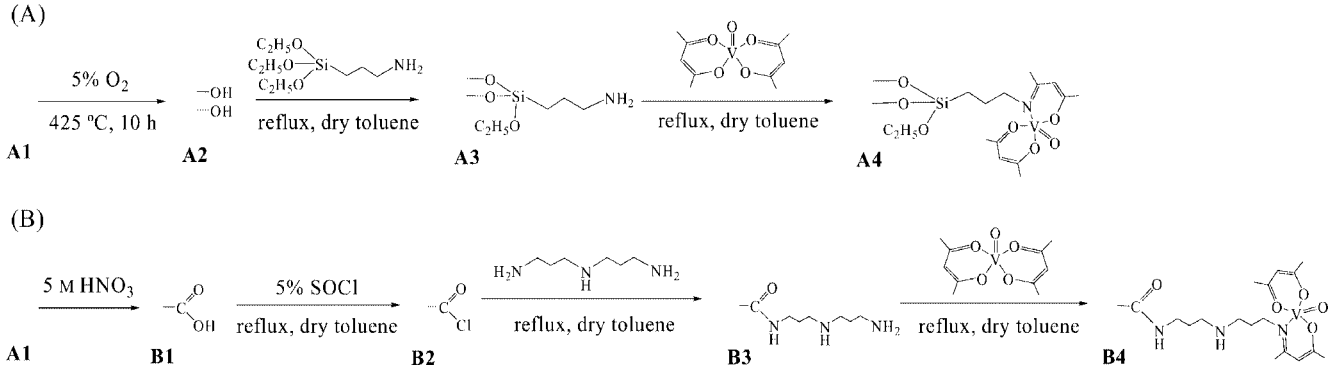

Scheme 1. Proposed structures for the anchored $[VO(acac)_2]$ on functionalised activated carbons prepared by methods A and B.

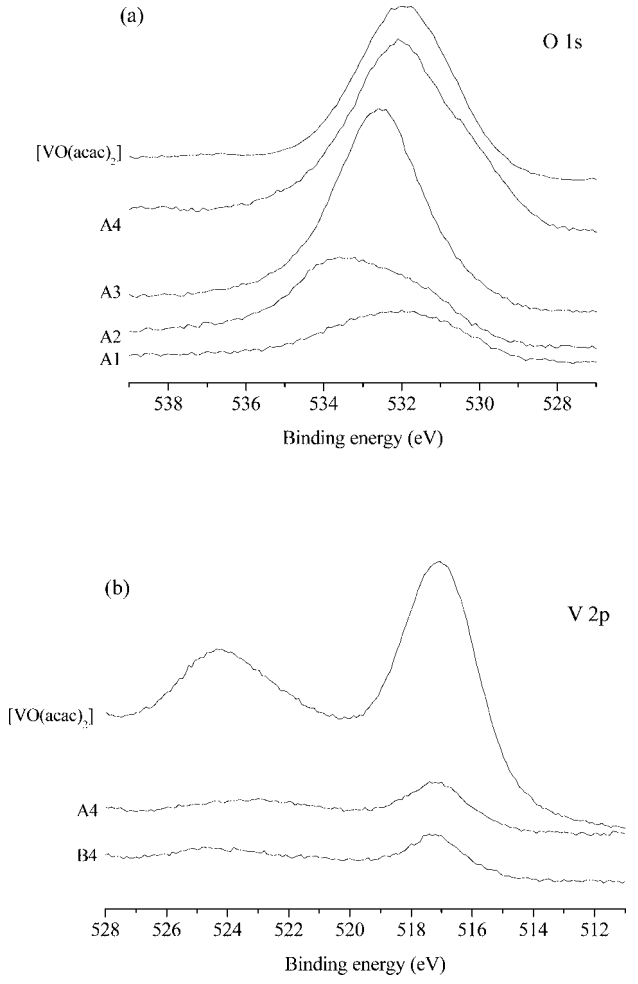

Figure 1. High-resolution XPS spectra of carbon-based materials in the O 1s (a) and V 2p (b) regions.

that APTES has been successfully anchored onto the air-oxidised carbon. The spectra of A3 in the O 1s region (Figure 1, a) is quite different from carbon A2 and shows a very intense and symmetric peak at 532.6 eV; this peak may be assigned not only to ether-type oxygen atoms, which result from the reaction between the APTES ethoxy functionalities and carbon surface phenol groups, but also to unreacted ethoxy groups from the aminoalkylsilane.[25,28] Upon complex anchoring on carbon A3, a new peak at 531.6 eV is observed in the O 1s region, which may be assigned to oxygen atoms from $[VO(acac)_2]$ (BE = 531.7 eV; Figure 1, a);[19–23] an increase in intensity in the high binding energies of the N 1s peak is also detected, suggesting the presence of nitrogen atoms in a new and different chemical environment.

Upon reaction of carbon B1 with thionyl chloride there is an increase in the chlorine content accompanied by a decrease in the oxygen content, thus indicating the formation of acyl chloride groups.[21,23] With the introduction of trien in B2, there is a significant increase in the nitrogen content, accompanied by a decrease in the chlorine surface quantity. This indicates that reaction between the amine groups of trien and the carbon acyl chloride functionalities has occurred, with formation of new amide groups and loss of hydrogen chloride. A loss of the surface oxygen is also observed, which can be explained by the parallel reaction of trien with other carbon surface groups, such as carbonyl groups, thus increasing the effectiveness of the trien anchoring.[23] Similarly, after reaction of B3 with $[VO(acac)_2]$, an increase in the peak at 532.0 eV in the O 1s region is observed (assigned to the oxygen atoms of the complex) and an increase in the broadness of the N 1s peak is also detected as a consequence of the presence of new nitrogen atoms in different chemical environments.

The observation of peaks in the V $2p_{3/2}$ region of the high-resolution spectra of A4 and B4 (Figure 1, b) confirms the presence of the metal complexes in both modified activated carbons. The areas under these bands allow the calculation of the surface amount of vanadium per weight of material, which are 697 and 554 $\mu mol\,g^{-1}$, respectively (Table 2). The similarity between the V 2p band profiles of the free and the anchored complexes (A4 and B4) suggests that the complex has kept its integrity upon immobilisation on the activated carbons. Furthermore, a comparison of the V $2p_{3/2}$ peak of free $[VO(acac)_2]$ (BE = 516.8 eV) with those of anchored complexes in A4 and B4 (BE = 517.0 and 517.2 eV, respectively; Figure 1, b) gives additional information on the V metal centre: the observed shift to higher binding energies suggests the presence of a more deshielded V centre. This observation, combined with the results referred to above, suggest complex anchoring through Schiff-base condensation between the carbon amine groups and ligand oxygen atoms, with the formation of a V–N in-plane bond, which induces a higher degree of in-plane covalence. Nonetheless, on the basis of the XPS data alone, we cannot exclude some direct axial coordination of the complex (available sixth position) onto the carbon oxygen surface

Table 2. Vanadium and silicon bulk contents obtained by ICP-AES.

Sample	Si [wt.-%]	n_i[a] [mmol g^{-1}]	n_f[b] [mmol g^{-1}]	η[c] [%]	V [wt.-%]	n_i[d] [μmol g^{-1}]	n_f[e] [μmol g^{-1}]	η[c] [%]
A4	3.00	1.42	1.10 (3.76)[f]	77	0.65	198	128 (697)[f]	65
B4	–	–	–	–	0.85	198	170 (554)[g]	86

[a] n_i = initial APTES mol (solution)/weight activated carbon. [b] n_f = adsorbed APTES mol/weight activated carbon. [c] $\eta = n_f \times 100/n_i$. [d] n_i = initial $[VO(acac)_2]$ mol (solution)/weight activated carbon. [e] n_f = adsorbed $[VO(acac)_2]$ mol/weight activated carbon. [f] Silicon surface content per weight of sample calculated from XPS data in Table 1: mmol Si/weight of sample = atom % Si/[atom % C × Ar(C) + atom % N × Ar(N) + atom % O × Ar(O) + atom % Si × Ar(Si) + atom % Cl × Ar(Cl) + atom % V × Ar(V)]. [g] Vanadium surface content per weight of sample calculated from XPS data in Table 1: μmol V/weight of sample = atom % V/[atom % C × Ar(C) + atom % N × Ar(N) + atom % O × Ar(O) + atom % Si × Ar(Si) + atom % Cl × Ar(Cl) + atom % V × Ar(V)].

groups, as a similar effect on the vanadium binding energy would be expected. The other hypothesis for complex anchoring via vanadium axial coordination through the free NH_2 groups of trien or APTES can be excluded, as it would induce an increase in V electronic density (NH_2 groups behave as electron donors), thus leading to a more shielded V atom, which would give rise to a decrease in the binding energy.

The vanadium bulk content of carbons A4 and B4 was determined by ICP-AES and from this it was possible to calculate the complex loading (mass of vanadium/mass of carbon × 100) and the immobilisation efficiency (amount of adsorbed complex/amount in original solution × 100), which are summarised in Table 2. In the case of material A4, the silicon bulk content was also obtained, allowing the calculation of APTES loading and its anchoring efficiency on carbon A4 (1.10 μmol g^{-1} and 77%, respectively). The complex is anchored more efficiently onto the trien-functionalised carbon (86%) than onto the APTES-functionalised carbon (65%).

The vanadium bulk contents for A4 and B4 are 128 and 170 μmol g^{-1}, respectively, and are therefore lower than the surface content obtained by XPS (697 and 554 μmol g^{-1}, respectively). This suggests that both vanadyl(IV) acetylacetonate complexes are mainly anchored at the outer pores of the carbon matrix (although this is more evident for material A4), probably as a consequence of size constraints imposed by the size of the innermost pores of the activated carbon. Similarly, the Si surface content in A3 is higher than that obtained by bulk analysis (3.76 and 1.10 mmol g^{-1}, respectively); this constitutes indirect evidence that the complex has been anchored preferentially onto the APTES sites within the activated carbon.

Electron Paramagnetic Resonance

The EPR spectra of A4 and B4 (Figure 2) are very similar and show a typical signal of V^{IV} $3d^1$ centres with eight-line hyperfine patterns due to the interaction of the unpaired electron with the ^{51}V nucleus (I = 7/2); the spectra are typical of magnetically diluted monomeric vanadyl ($V{=}O^{2+}$) species with g values and vanadium hyperfine coupling constants characteristic of a square-pyramidal structure with approximate axial geometry;[29–31] this indicates that there is no significant magnetic interactions between vicinal V centres and that the carbon matrix acts as a diamagnetic host.

The similarity between the EPR spectra of A4 and B4 with those observed for the free VO complexes[29–31] allows the same orientation scheme to be used for the tensor axes: $g_1 = g_2 = g_\perp$, $g_3 = g_\parallel$ (or $g_1 = g_x$, $g_2 = g_y$, $g_3 = g_z$), where g_1 and g_3 refer to the lowest and highest magnetic-field g values (obviously, $A_1 = A_2 = A_\perp$, $A_3 = A_\parallel$ or $A_1 = A_x$, $A_2 = A_y$, and $A_3 = A_z$); in this context, as $g_x = g_y > g_z$ the ground state is d^1_{xy}. The EPR spectra of A4 and B4 are presented in Figure 2, and the spin-Hamiltonian parameters for free $[VO(acac)_2]$ magnetically diluted in KBr and the carbon-anchored complexes are summarised in Table 3.

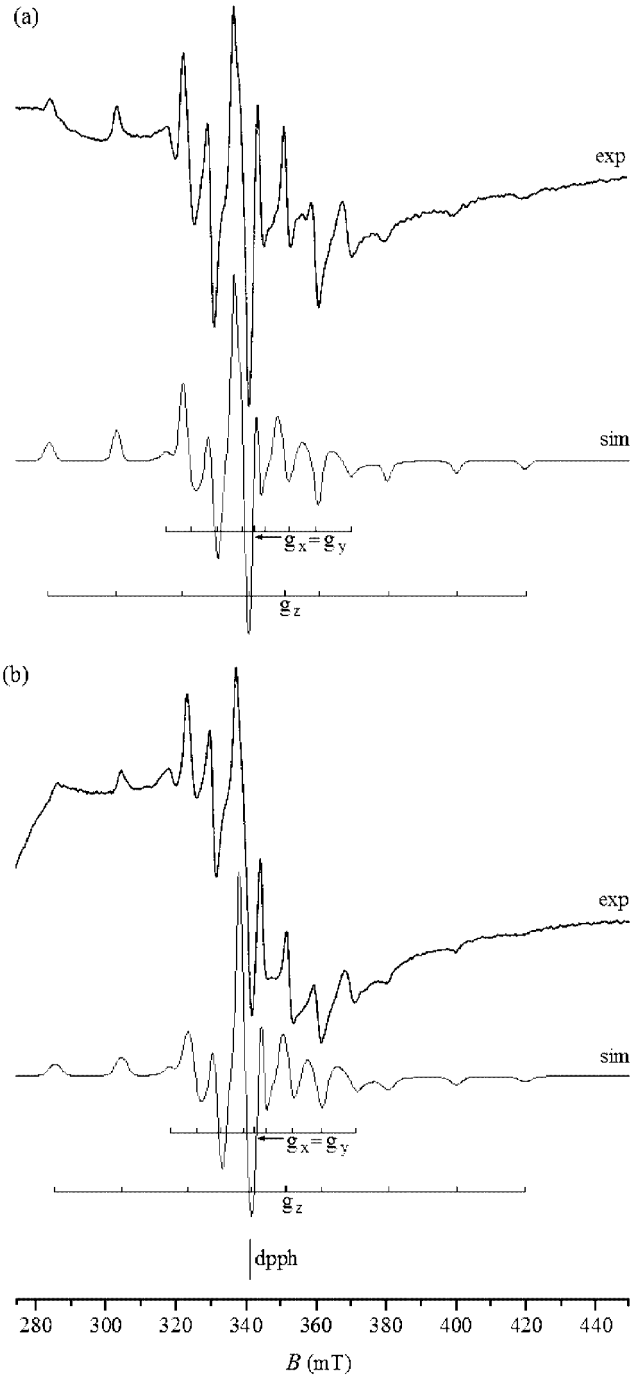

Figure 2. EPR spectra (ν = 9.57 GHz) for carbon B4 at 125 K (a) and carbon A4 at 165 K (b) (exp = measured, sim = simulated).

Table 3. Spin-Hamiltonian parameters for the free and supported $[VO(acac)_2]$ complex.

Sample	$g_\perp$	$g_\parallel$	$A_\perp$[a]	$A_\parallel$[a]	g_{av}[b]	A_{av}[a,c]
$[VO(acac)_2]$[d]	1.986	1.944	71	177	1.972	106
A4	1.984	1.937	71	173	1.968	105
B4	1.987	1.944	70	176	1.973	105

[a] Units of hyperfine coupling constants: $\times 10^{-4}$ cm^{-1}. [b] $g_{av} = 1/3(2\times g_\perp + g_\parallel)$. [c] $A_{av} = 1/3(2\times A_\perp + A_\parallel)$. [d] Powered sample magnetically diluted in KBr: 0.085 mmol $[VO(acac)_2]$ in 0.5 g KBr.

The EPR band profile of both materials indicates that there is only one major VO EPR active species within the carbon matrix (small bandwidth and no additional peaks besides those that are predicted for one species) and corroborates the V 2p XPS data. Both materials, when compared to the free complex, show a decrease in $A_{\parallel}$, although this is quite small for B4, suggesting a decrease in the unpaired spin density at the V centre upon carbon anchoring. This excludes the axial coordination of APTES or trien through the NH_2 functionalities, as this would increase the $A_{\parallel}$ values. In the light of the model developed by Wuthrich and refined later by Chasteen,[29,30,32] this result can be interpreted as an increase in the in-plane covalency: in our context, complex anchoring through the Schiff-base condensation between amine functionalities from trien or APTES and the acetylacetone ligand would lead to a new in-plane V–N bond, which would increase the delocalisation of the electron density towards the equatorial ligand, thus inducing a decrease in $A_{\parallel}$. Although new equatorial V–N bonds would give rise to the appearance of superhyperfine splittings due to the interaction of the vanadium unpaired spin with the equatorial nitrogen atom ($I = 1$; d_{xy} ground state), no splitting due to the presence of N atoms could be detected in the EPR spectra, probably due to the relatively big bandwidth that is associated with solid-state spectra.

Parallel with the decrease in $A_{\parallel}$, an increase in $g_{\parallel}$ (towards the g_e value) is usually observed as a consequence of the increase in the equatorial bonding covalence.[30–32] However, our data do not follow this trend, since no variation in the g values is observed for B4 and a decrease in g values is detected for A4 when compared to free $[VO(acac)_2]$. Nonetheless, these results do not contradict the above explanations as strong distortions of the anchored complexes within the matrix are expected to occur and, under this circumstances, the g values can show dissimilar changes upon complex distortion:[30] the g_z values are usually insensitive to the degree of the distortion of complex structure, whereas g_x and g_y exhibit a greater variation, although in an unpredicted random manner.

No characterisation of the material is possible by FTIR and UV/Vis spectroscopy in order to get further information on complex distortion induced by the anchoring procedure, as the strongly absorbing carbon matrix prevents the observation of the typical complex responses. Although EPR spectra could not give straightforward evidence for the molecular structure of the anchored complexes, a combination of all the data allowed us to propose the anchoring of $[VO(acac)_2]$ onto the amine-functionalised carbons via Schiff-base condensation with the acetylacteonate ligand, as summarised in Scheme 1.

Further indirect information on the complex anchoring can be gained by the assessment of the heterogeneous catalytic activity of the new materials in a typical reaction where the homogeneous $[VO(acac)_2]$ complex shows high catalytic performance. In fact, the catalytic activity of a homogeneous catalyst (reaction conversion and products yields) is only kept upon its heterogenisation when no significant changes occur in the coordination sphere of the active centre, namely coordination atoms and available coordination sites for the substrate. In this context, we studied the catalytic activity of $[VO(acac)_2]$ towards the epoxidation of an allylic alcohol after immobilisation on the functionalised activated carbon.

Epoxidation of 3-Buten-2-ol Catalysed by Heterogeneous [VO(Acac)$_2$] Catalysts

The results obtained in the epoxidation of 3-buten-2-ol at 0 °C using vanadyl(IV) acetylacetonate based materials as heterogeneous catalysts and *tert*-butyl hydroperoxide as the oxygen source, in dichloromethane, are summarised in Table 4 and in Figure 3; data from the homogeneous phase and a blank experiment run under identical conditions are also included.

Table 4. Epoxidation of 3-buten-2-ol at 0 °C catalysed by $[VO(acac)_2]$ in homogeneous and heterogeneous phase.[a]

Catalyst	Time [h]	Cycle	Conversion[b] [%]	TON[c]	TOF[d] [h^{-1}]
$[VO(acac)_2]$	1	1st	2	1	1.0
	2	1st	5	3	1.5
	24	1st	56	29	1.2
	27	1st	59	31	1.2
	51	1st	90	47	0.9
	76	1st	93	49	0.6
A1 (blank)	24	1st	9	–	–
	48	1st	18	–	–
	72	1st	24	–	–
	144	1st	46	–	–
A4	24	1st	18	9	0.4
	48	1st	49	25	0.5
	72	1st	76	38	0.5
	144	1st	100	50	0.4
	144	2nd	94	48	0.3
B4	24	1st	3	2	0.08
	48	1st	9	5	0.1
	72	1st	20	11	0.2
	192	1st	100	53	0.3
	192	2nd	94	48	0.2

[a] Typical reaction conditions used: 0.850 mmol of 3-buten-2-ol, 0.425 mmol of chlorobenzene (internal standard), 0.017 mmol of $[VO(acac)_2]$ or 0.100 g of heterogeneous catalyst (2% of catalyst relative to 3-buten-2-ol), 1.70 mmol of *t*BuOOH. [b] Based on 3-buten-2-ol consumption. [c] TON = mmol of converted 3-buten-2-ol/mmol of vanadium. [d] TOF = TON/reaction time.

The 3-buten-2-ol conversion was approximately 100% in both heterogeneous-phase reactions, with total TONs slightly higher than the homogeneous-phase reaction, thus indicating that the catalyst conversion performances did not decrease upon heterogenisation of $[VO(acac)_2]$. The high catalytic activity of the new vanadium-based materials clearly supports the proposed structure for complexes being anchored by the ligand and not through axial coordination (spacers or carbon surface oxygen groups), which would result in a six-coordinate species without an available coordination site for the oxidant. Therefore, the axial coordination would hinder the formation of the active intermediate V species (peroxovanadium intermediate),[8] leading to inactive anchored V complexes.

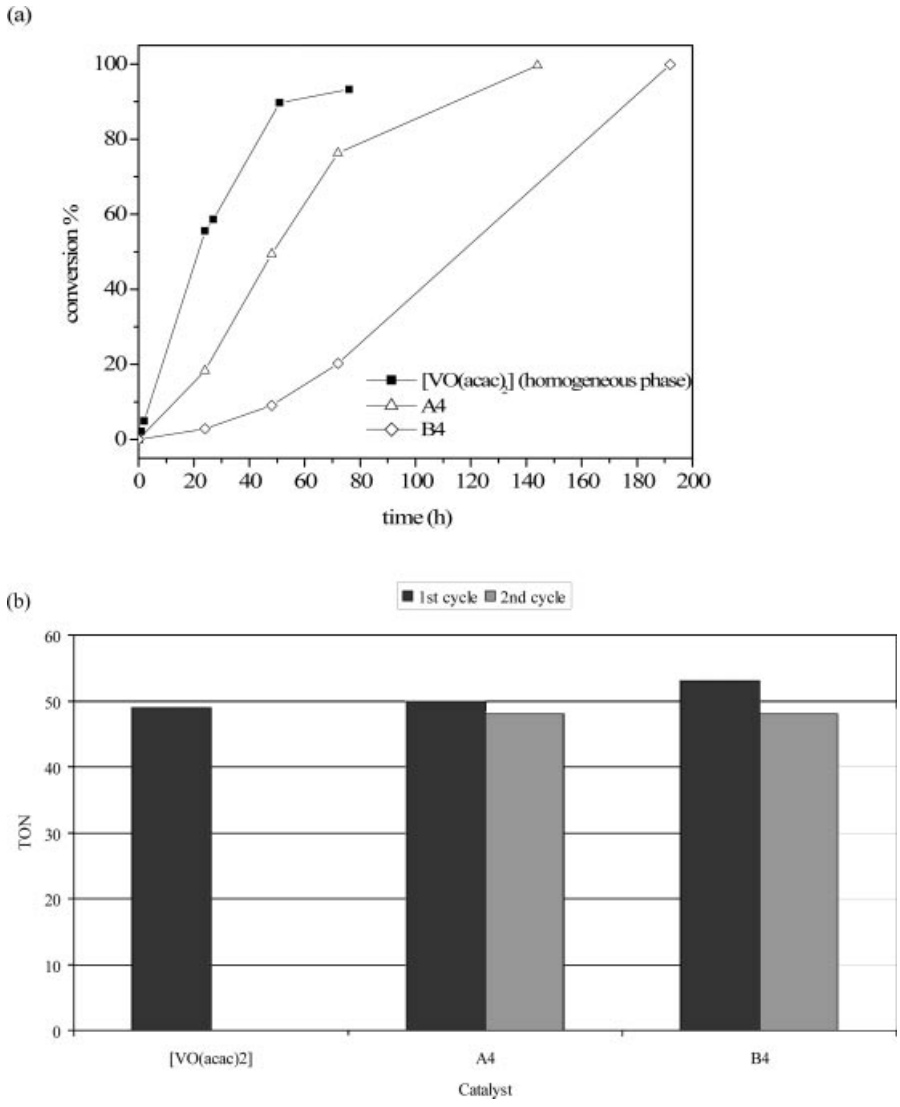

Figure 3. Epoxidation of 3-buten-2-ol catalysed by the $[VO(acac)_2]$ complex in the homogeneous phase and heterogenised onto two different functionalised activated carbons (A4 and B4): (a) conversion vs. time and (b) TON vs. catalyst.

However, on going from the homogeneous to the heterogeneous phase, an increase in the reaction time is observed in both heterogeneous catalyst runs under identical reaction conditions. This is a general effect that arises upon immobilisation of metal complexes in porous matrices, and has been attributed to diffusion constraints imposed on substrates and reactants by the porous network of the matrices.[20] As the catalytic conversions of the immobilised complexes are similar to that of free $[VO(acac)_2]$, we propose the same justification for the observed increase in the reaction time.

Comparing the two epoxidation reactions using A4 and B4 as heterogeneous catalysts, it can be observed that the former proceeds more rapidly in the initial 72 hours, a result that can be directly associated with the more external location of the metal complex in material A4, which lessens diffusion constraint effects.

Reutilisation is one of the greatest advantages of heterogeneous catalysts, and can also provide useful information about the anchoring process and catalyst stability along the catalytic cycle. As can be seen in Table 4 and in Figure 3, it is clear that neither A4 nor B4 lose their catalytic efficiency significantly after two catalytic cycles. This is an important result for heterogeneous vanadium-based catalysis and indicates that the two anchoring procedures are very effective at preventing complex deactivation and leaching, at least up to two cycles.

Concluding Remarks

New heterogeneous catalysts were prepared by heterogenisation of $[VO(acac)_2]$ onto amine-functionalised activated carbons prepared by two different methodologies: (a) using an air-oxidised carbon functionalised with APTES and (b) using an acid-oxidised carbon functionalised with trien. The combination of XPS and EPR data showed that complex anchoring was achieved by Schiff-base condensa-

tion between the free amine groups of the functionalised carbon and the oxygen ligand atoms. These new vanadium-based materials show high catalytic activity in the epoxidation of 3-buten-2-ol and are not very different from $[VO(acac)_2]$ (conversion and TON), which corroborates the proposed anchoring methodologies. Material A4 proved to be a more efficient catalyst, as can be seen by its greater values of TON in the first 72 hours. Both materials were used two times with no significant loss in the alkene conversion and TON, thus indicating that the complexes have been anchored irreversibly to the carbon surface, which prevents leaching of the active phase and its deactivation.

Experimental Section

Materials and Solvents: The starting carbon material was a NORIT ROX 0.8 activated carbon (rodlike pellets with 0.8 mm diameter and 5 mm length). This material has a pore volume of 0.695 $cm^3 g^{-1}$, as determined by porosimetry (corresponding to meso- and macropores), a micropore volume of 0.359 $cm^3 g^{-1}$ and a mesopore area of 122 $m^2 g^{-1}$, as determined by N_2 adsorption at 77 K (*t*-method),[19–23] an ash content of 2.6% (w/w), an iodine number of 1000 and mercury and helium densities of 0.666 and 2.11 $g cm^{-3}$, respectively. The activated carbon was purified by Soxhlet extraction with 2 M HCl for 6 h, washed with deionised water until pH 6–7 and then dried in an oven at 150 °C for 13 h under vacuum (A1).

(3-Aminopropyl)triethoxysilane, bis(3-aminopropyl)amine, vanadyl(IV) acetylacetonate, a *tert*-butyl hydroperoxide solution in decane (5 M), chlorobenzene and 3-buten-2-ol were obtained from Aldrich and were used as received. All the reagents and solvents used in the modification of the activated carbon and in the anchoring procedure were also obtained from Aldrich, except for ethanol, toluene and thionyl chloride, which were purchased from Merck (pro analysi). The reagents and solvents used in the catalytic experiments were obtained from Aldrich, except for dichloromethane, which was purchased from Romil (HPLC grade).

$[VO(acac)_2]$: XPS (eV): C 1s 285.0 and 287.1; O 1s 531.7; V $2p_{3/2}$ 516.8.

Preparation of the Heterogeneous Catalysts: The immobilisation of the vanadium complex was performed by two different methods, A and B, that are described below and summarised in Scheme 1.

Support Oxidation: The activated carbon (A1) was oxidised by two methods:[22,23] (a) with a mixture of N_2 and air (5% O_2) at 698 K for 10 h (A2; burn-off = 11%), (b) refluxed with a 5 M nitric acid solution for 6 h (1 g/30 mL), washed with deionised water until pH 6–7 and then dried in an oven at 110 °C for 13 h under vacuum (B1). Carbon A2 was used as the support for the complex anchoring by method A whereas carbon B1 was used as support for method B.

Method A. Functionalisation of A2 with (3-Aminopropyl)triethoxysilane (APTES): Carbon A2 (3.0 g) was refluxed with a solution containing 4.3 mmol of (3-aminopropyl)triethoxysilane in 100 mL of dry toluene for 24 h, then filtered and washed extensively with dry toluene. The material was Soxhlet extracted for 8 h with toluene and 8 h with ethanol and was then dried in an oven at 120 °C for 13 h under vacuum (carbon A3).

Anchoring of $[VO(Acac)_2]$ onto the A3 Carbon: The activated carbon functionalised with (3-aminopropyl)triethoxysilane (A3, 0.60 g) was added to 100 mL of a solution of $[VO(acac)_2]$ in dry toluene (118 μmol), and the mixture was refluxed for 9 h; during the reflux a progressive disappearance of the green colour of the solution was observed. The resulting material was extensively washed with toluene and then purified by Soxhlet extraction with toluene for 8 h, and dried in an oven at 120 °C for 13 h under vacuum (carbon A4).

Method B. Reaction of B1 with Thionyl Chloride ($SOCl_2$): Carbon B1 (12.0 g) was refluxed with 40 mL of a 5% (v/v) solution of thionyl chloride in toluene for 5 h, extensively washed with toluene, and then purified by Soxhlet extraction with toluene for 2 h, and finally dried in an oven at 150 °C for 13 h under vacuum (carbon B2).[23]

Functionalisation of B2 with Bis(3-aminopropyl)amine (Trien): Carbon B2 (3.0 g) was refluxed with a solution containing 390 μmol of bis(3-aminopropyl)amine (trien) in 40 mL of dry toluene for 4 h, then filtered and extensively washed with toluene. The material was also Soxhlet extracted for 2 h with toluene and dried in an oven at 150 °C for 13 h under vacuum (carbon B3).[23]

Anchoring of $[VO(Acac)_2]$ onto the B3 Carbon: The activated carbon functionalised with trien (B3, 0.60 g) was added to 100 mL of a solution of $[VO(acac)_2]$ in dry toluene (119 μmol), and the mixture was refluxed for 9 h; during the reflux a progressive disappearance of the green colour of the solution was observed. The resulting material was extensively washed with toluene and then purified by Soxhlet extraction with toluene for 7 h, and dried in an oven at 150 °C for 13 h under vacuum (carbon B4).

Physical Measurements: Vanadium and silicon bulk contents were obtained by inductively coupled plasma emission spectrometry (ICP-AES) at "Laboratório de Análises", IST, Lisboa (Portugal). X-ray photoelectron spectroscopy (XPS) was performed at "Centro de Materiais da Universidade do Porto" (Portugal), with a VG Scientific ESCALAB 200A spectrometer using non-monochromated Mg-K_α radiation (1253.6 eV). In order to correct for possible deviations caused by the electric charge of the samples, the graphitic C 1s band at 284.6 eV was taken as internal standard.[33,34] EPR spectra were obtained with an X-band Bruker ESP 300E spectrometer. The powdered samples were diluted in KBr (5%), the microwave frequency was calibrated with diphenylpicrylhydrazyl (dpph; g = 2.0037) and the magnetic field was calibrated against Mn^{II} in MgO. Experimental conditions: modulation frequency: 100 kHz; modulation amplitude: 9 G; microwave power: 1 mV. The EPR parameters were obtained by simulation using the program WINEPR SimFonia (Bruker) by assuming axial spin-Hamiltonians. The line widths used in the simulations were 15–30 G. Gas chromatography experiments (GC) were performed with a Varian CP-3380 chromatograph equipped with an FID detector and using helium as carrier gas and a fused silica Varian Chrompack capillary column CP-Sil 8 CB Low Bleed/MS (30 m × 0.25 mm i.d.; 0.25 μm film thickness). The chromatographic conditions were: 40 °C (3 min), 5 °C min^{-1} to 170 °C (2 min), 20 °C min^{-1} to 200 °C (10 min); injector temperature: 200 °C; detector temperature: 300 °C. Aliquots of 0.1 mL were withdrawn from the reaction mixture with a hypodermic syringe, filtered through PTFE 0.22-μm syringe filters and injected directly into the injector using a 1-μL Hamilton syringe.

Catalysis Experiments: The reactions were carried out in CH_2Cl_2, at 0 °C, with constant stirring. The composition of the reaction medium was 0.85 mmol of 3-buten-2-ol, 0.425 mmol of chlorobenzene (internal standard), 0.10 g of heterogeneous catalyst (A4 or B4) in 5.00 mL of solvent. The oxidant, *tert*-butyl hydroperoxide (1.70 mmol), was progressively added to the reaction medium using a Bioblock Scientific Syringe Pump at a rate of 0.5 mL h^{-1}. For

each complex the reaction time for maximum conversion percentage was determined by withdrawing 0.1-mL aliquots periodically from the reaction mixture, and this time was used to monitor the efficiency of the catalyst. The composition of the reaction media was determined by GC with 3-buten-2-ol, *tert*-butyl hydroperoxide, *tert*-butanol and decane being quantified by the internal standard method (chlorobenzene). The catalysts were then washed sequentially by Soxhlet extraction with 100 mL of toluene and 100 mL of ethanol for 1–2 hours, and dried at an oven at 120 °C for 13 h, under vacuum. The catalysts were then reused using the same experimental conditions. Control experiments using the initial carbon A1 and the homogeneous reaction with vanadyl(IV) acetylacetonate in identical reaction conditions were also performed.

Acknowledgments

The authors are indebted to Dr. Carlos Sá (CEMUP) for assistance with XPS analysis and to NORIT N.V., Amersfoort, Netherlands, for providing the activated carbon. This work was partially funded by the Fundação para a Ciência e a Tecnologia (FCT, Portugal) and FEDER through project ref. POCTI/EQU/57369/2004. ARS thanks FCT and the European Social Fund for a postdoctoral fellowship.

[1] V. Conte, F. Di Furia, G. Licini, *Appl. Catal., A* **1997**, *157*, 335–361.
[2] C. Bolm, *Coord. Chem. Rev.* **2003**, *237*, 245–256.
[3] S. Raghavan, A. Rajander, S. C. Joseph, *Synth. Commun.* **2001**, *31*, 1477–1480.
[4] M. Kirihara, M. Ichinose, S. Takisawa, *Chem. Commun.* **1998**, 1691–1692.
[5] T. Okada, M. Ueda, *React. Funct. Polym.* **1996**, *30*, 157–163.
[6] K. Yamamoto, E. Tsuchida, H. Nishide, *Macromolecules* **1993**, *26*, 3432–3437.
[7] T. Katsuki, *Coord. Chem. Rev.* **1995**, *140*, 189–214.
[8] B. E. Rossiter, T. R. Verhoeven, K. B. Sharpless, *Tetrahedron Lett.* **1979**, *20*, 4733–4736.
[9] A. G. J. Ligtenbarg, R. Hage, B. L. Feringa, *Coord. Chem. Rev.* **2003**, *237*, 89–101.
[10] L. Canali, D. C. Sherrington, *Chem. Soc. Rev.* **1999**, *28*, 85–93.
[11] Q.-H. Fan, Y.-M. Li, A. S. C. Chan, *Chem. Rev.* **2002**, *102*, 3385–3466.
[12] N. E. Leadbeater, M. Marco, *Chem. Rev.* **2002**, *102*, 3217–3274.
[13] D. Brunel, N. Belloq, P. Sutra, A. Cauvel, M. Laspéras, P. Moreau, F. Di Renzo, A. Galarneau, F. Fajula, *Coord. Chem. Rev.* **1998**, *178–180*, 1085–1108.
[14] F. Rodríguez-Reinoso, *Carbon* **1998**, *36*, 159–175.
[15] A. J. Bird, in *Catalyst Supports and Supported Catalysts* (Ed.: A. B. Stiles), Butterworths, Boston, **1987**, chapter 5.
[16] P. C. L'Argentière, E. A. Cagnola, D. A. Liprandi, M. C. Román-Martínez, C. Salinas-Martínez de Lecea, *Appl. Catal., A* **1998**, *172*, 41–48.
[17] J. A. Díaz-Auñón, M. C. Román-Martínez, C. Salinas-Martínez de Lecea, P. C. L'Argentière, E. A. Cagnola, D. A. Liprandi, M. E. Quiroga, *J. Mol. Catal. A: Chem.* **2000**, *153*, 243–256.
[18] J. A. Díaz-Auñón, M. C. Román-Martínez, C. Salinas-Martínez de Lecea, *J. Mol. Catal. A: Chem.* **2001**, *170*, 81–93.
[19] A. R. Silva, M. M. A. Freitas, C. Freire, B. de Castro, J. L. Figueiredo, *Langmuir* **2002**, *18*, 8017–8024.
[20] A. R. Silva, J. L. Figueiredo, C. Freire, B. de Castro, *Microporous Mesoporous Mater.* **2004**, *68*, 83–89.
[21] A. R. Silva, M. Martins, M. M. A. Freitas, A. Valente, C. Freire, B. de Castro, J. L. Figueiredo, *Microporous Mesoporous Mater.* **2002**, *55*, 275–284.
[22] A. R. Silva, C. Freire, B. de Castro, M. M. A. Freitas, J. L. Figueiredo, *Microporous Mesoporous Mater.* **2001**, *46*, 211–221.
[23] A. R. Silva, M. Martins, M. M. A. Freitas, J. L. Figueiredo, C. Freire, B. de Castro, *Eur. J. Inorg. Chem.* **2004**, 2027–2035.
[24] J. L. Figueiredo, M. F. R. Pereira, M. M. A. Freitas, J. J. M. Órfão, *Carbon* **1999**, *37*, 1379–1389.
[25] A. M. Yacynych, T. Kuwana, *Anal. Chem.* **1978**, *50*, 640–645.
[26] Z. R. Yue, W. Jiang, L. Wang, S. Gardner, C. U. Pittman Jr., *Carbon* **1999**, *37*, 1785–1796.
[27] E. Desimoni, G. I. Casella, A. M. Salvi, *Carbon* **1992**, *30*, 521–526.
[28] M. F. Dautartas, J. F. Evans, T. Kuwana, *Anal. Chem.* **1979**, *51*, 104–110.
[29] A. J. Tasiopoulos, A. N. Troganis, A. Evangelou, C. P. Raptopoulou, A. Terzis, Y. Deligiannakis, T. A. Kabanos, *Chem. Eur. J.* **1999**, *5*, 910–921.
[30] E. Garribba, G. Micera, A. Panzanelli, D. Sanna, *Inorg. Chem.* **2003**, *42*, 3981–3987.
[31] E. J. Tolis, V. I. Teberekidis, C. P. Raptopoulou, A. Terzis, M. P. Sigalas, Y. Deligiannakis, T. A. Kabanos, *Chem. Eur. J.* **2001**, *7*, 2698–2710.
[32] T. S. Smith II, R. LoBrutto, V. L. Pecoraro, *Coord. Chem. Rev.* **2002**, *228*, 1–18.
[33] J. F. Moulder, W. F. Stickle, P. E. Sobol, K. D. Bomben, in *Handbook of X-ray Photoelectron Spectroscopy* (Ed.: J. Chastain), Perkin–Elmer, **1992**.
[34] Y. M. Xie, P. M. A. Sherwood, *Chem. Mater.* **1990**, *2*, 293–299.

Received: May 12, 2005
Published Online: October 10, 2005

